

See discussions, stats, and author profiles for this publication at: <https://www.researchgate.net/publication/297680394>

The effect of Na_3FeF_6 catalyst on the hydrogen storage properties of MgH_2

Article in Dalton Transactions · March 2016

DOI: 10.1039/C6DT00068A

CITATIONS

4

READS

44

3 authors, including:



Nurul Shafikah Mohd Mustafa
Universiti Malaysia Terengganu

3 PUBLICATIONS 5 CITATIONS

[SEE PROFILE](#)



Mohammad Ismail
Universiti Malaysia Terengganu

40 PUBLICATIONS 590 CITATIONS

[SEE PROFILE](#)

Some of the authors of this publication are also working on these related projects:



MgH₂+PdCl₂ [View project](#)

All content following this page was uploaded by [Mohammad Ismail](#) on 21 April 2016.

The user has requested enhancement of the downloaded file. All in-text references [underlined in blue](#) are added to the original document and are linked to publications on ResearchGate, letting you access and read them immediately.

CrossMark
click for updatesCite this: *Dalton Trans.*, 2016, **45**,
7085

Effect of Na₃FeF₆ catalyst on the hydrogen storage properties of MgH₂

N. N. Sulaiman, [N. S. Mustafa](#) and [M. Ismail*](#)

The effects of Na₃FeF₆ catalyst on the hydrogen storage properties of MgH₂ have been studied for the first time. The results showed that for the MgH₂ sample doped with 10 wt% Na₃FeF₆, the onset dehydrogenation temperature decreased to 255 °C, which was 100 °C and 162 °C lower than those of the as-milled and as-received MgH₂ sample, respectively. The re/dehydrogenation kinetics were also significantly enhanced compared to the un-doped MgH₂. The absorption kinetics showed that the as-milled MgH₂ only absorbed 3.0 wt% of hydrogen at 320 °C in 2 min of rehydrogenation, but about 3.6 wt% of hydrogen was absorbed within the same period of time after 10 wt% Na₃FeF₆ was added to MgH₂. The desorption kinetics showed that the MgH₂ + 10 wt% Na₃FeF₆ sample could desorb about 3.8 wt% of hydrogen in 10 min at 320 °C. In contrast, the un-doped MgH₂ sample desorbed only 0.2 wt% of hydrogen in the same period of time. The activation energy for the decomposition of the as-milled MgH₂ was 167.0 kJ mol⁻¹, and this value decreased to 75.0 kJ mol⁻¹ after the addition of 10 wt% Na₃FeF₆ (a reduction by about 92.0 kJ mol⁻¹). It is believed that the *in situ* formation of the active species of NaMgF₃, NaF and Fe during the heating process could enhance the hydrogen storage properties of MgH₂, due to the catalytic effects of these new species.

Received 11th January 2016,
Accepted 6th March 2016

DOI: 10.1039/c6dt00068a

www.rsc.org/dalton

1. Introduction

Hydrogen is a clean and safe energy carrier and has significant potential for use as an environmentally friendly energy carrier in future applications. Since hydrogen reacts with oxygen and produces water vapor as the exhaust in fuel cell applications, it is considered to be pollution-free. This correlates with the target formulated by the US Department of Energy (DOE)¹ for a long-term vision for the applications of hydrogen storage that considers the economic and environmental parameters. Although hydrogen has the potential to be an energy carrier, the main problems faced are how to store and release it. There are three approaches to storing hydrogen: storing it at high pressures, cryogenics, and in the solid-state. The solid state hydrogen storage was chosen rather than the cryogenic liquid and gaseous states, due to several advantages such as the efficiency of energy, safety, and the effectiveness of cost.²

Metal hydrides,^{3–5} complex hydrides,^{6–11} carbon materials,¹² and metal–organic frameworks (MOFs)¹³ are the types of solid-state hydrogen storage materials that have been studied. Among the many types of solid-state hydrogen storage, MgH₂ is considered to be one of the most promising

materials due to its high hydrogen capacity (7.6 wt%), with the added advantages of being low cost and having superior reversibility.¹⁴ However, problems such as high decomposition temperature and slow desorption/absorption kinetics have dampened the hope of its commercialization.¹⁵ These disadvantages have been overcome by reducing the particle size,¹⁶ doping with catalysts,^{17–23} and reacting with other metals or metal hydrides (destabilization concept).^{24–28} Many studies have claimed that the fast and effective dissociation of hydrogen molecules was enabled by the enhancement of the hydrogen sorption kinetics in the metal hydride systems caused by catalytic factors.²⁹ Thus, the introduction of various catalysts into MgH₂ could enhance the hydrogenation properties of MgH₂.

To date, no research has been conducted to study the effects of Na₃FeF₆ as a catalyst on the hydrogenation performance of MgH₂. Na₃FeF₆, which contains Na, Fe and F species, may be an effective approach to enhancing the hydrogenation performance of MgH₂. Li, Be, Na, Mg, B and Al are light metals that could form a large variety of metal–hydrogen compounds.¹ These elements are quite attractive due to their light weight and the number of hydrogen atoms per metal atom. Moreover, NaAlH₄ is one of the promising alanates for practical application purposes because it was found to reversibly store 3–4 wt% hydrogen under moderate conditions by the addition of a small amount of Ti as a catalyst.³⁰ On the other hand, the hydrogen desorption properties of MgH₂ were also enhanced after being mixed with NaAlH₄.^{31,32} The onset

School of Ocean Engineering, Universiti Malaysia Terengganu, 21030 Kuala Terengganu, Malaysia. E-mail: mohammadismail@umt.edu.my; Fax: +609-6683991; Tel: +609-6683487

dehydrogenation temperature was significantly improved as it started to release hydrogen at about 280 °C, reduced by about 50 °C compared to as-milled MgH_2 . There was also an enhancement in the dehydrogenation kinetics.

Many studies have reported transition-metal compounds as effective catalysts for MgH_2 , resulting from the high affinity of transition-metal cations for hydrogen.^{33–35} Liang *et al.*³⁵ reported that the de/rehydrogenation kinetics of MgH_2 were enhanced by adding 5 wt% transition metal (Ti, V, Mn, Fe, and Ni) compared to un-doped MgH_2 . Recently, numerous studies have revealed that the reduction of the dehydrogenation temperature of metal hydrides and complex hydrides is due to the catalytic effects of the F-anion.^{36–39} Na based halides such as NaF have also been proven to be good catalysts for metal hydrides and alanates.^{40,41} It was reported that NaF particles work as nucleation centers for the formation of NaH, due to their identical crystallographic structures and comparable lattice parameters, which promote the nucleation and growth of NaH in the dehydrogenation process.⁴² It would therefore be quite reasonable and interesting to combine Na, Fe and F species to form a catalyst that would be able to have positive effects on the dehydrogenation of MgH_2 . To the best of the authors' knowledge, no research has been reported on MgH_2 doped with Na_3FeF_6 . In this study, the hydrogen storage performance of $\text{MgH}_2\text{-Na}_3\text{FeF}_6$ composite was studied using pressure-composition-temperature (PCT), differential scanning calorimetry (DSC), X-ray diffraction (XRD) and scanning electron microscopy (SEM). The possible catalytic mechanism from the results obtained is also discussed in this study.

2. Experimental details

MgH_2 (hydrogen storage grade, 98% purity) and Na_3FeF_6 were purchased from Sigma Aldrich. Both materials were used as received with no further purification or pretreatment. Approximately 150 mg of MgH_2 was ball-milled with different percentages (10 wt%, 20 wt%, and 50 wt% of the total substance amount) of Na_3FeF_6 . The samples were loaded into a sealed stainless steel vial, together with four hardened stainless steel balls. The ratio of the weight of the balls to the weight of the powder was 40 : 1. MgH_2 with different Na_3FeF_6 powder ratios were then milled for 1 h in a planetary ball mill (NQM-0.4), by first milling for 15 min, resting for 2 min and then milling for another 15 min in a different direction at the rate of 400 rpm for 2 cycles. For comparison, pure MgH_2 was also prepared under the same conditions. To eliminate the influence of oxygen and water moisture, all handling of the samples was performed in an MBraun Unilab glove box under high purity argon atmosphere.

The experiments on the temperature-programmed-desorption (TPD) and the de/rehydrogenation kinetics were performed in a Sievert-type pressure-composition-temperature (PCT) apparatus (Advanced Materials Corporation), also known as the Gas Reaction Controller (GRC). The samples were loaded into sample vessels in the glove box. For the TPD experiments, all the samples were heated in a vacuum

chamber and the lowest decomposition temperature of each sample was determined by measuring the amount of desorbed hydrogen. The samples were heated from room temperature to 450 °C with the heating rate of 5 °C min^{-1} . The de/rehydrogenation kinetics experiments were conducted at the desired temperature with the initial hydrogen pressures of 1.0 atm and 33.0 atm, respectively.

Differential scanning calorimetry (DSC) analysis of the as-prepared powder samples was carried out using a Mettler Toledo TGA/DSC 1. About 2–6 mg of the sample was loaded into an alumina crucible in the glove box. Subsequently, the crucible was placed in a sealed glass bottle in order to prevent oxidation during the transfer from the glove box to the DSC apparatus. An empty alumina crucible was used as reference. The samples were heated from room temperature to 500 °C under Ar atmosphere, and the heating rate was 20 °C min^{-1} .

XRD analysis was performed using a Rigaku MiniFlex X-ray diffractometer with Cu $K\alpha$ radiation. Before the measurement, a small amount of sample was spread uniformly on the sample holder and covered with a scotch tape, then sealed in a plastic wrap to prevent oxidation. The XRD analyses of the samples before and after desorption, as well as after rehydrogenation, were carried out at a speed of 2.00° min^{-1} over the diffraction angles from 20° to 80°. Moreover, the surface morphology of the samples was characterized using a scanning electron microscope (SEM; JEOL JSM-6360LA). The samples were prepared on a carbon tape and then coated with gold spray under a vacuum. In order to minimize the oxidation, the preparations of the samples were also carried out in the glove box.

3. Results and discussion

Fig. 1 displays the temperature programmed desorption (TPD) performances of the as-received MgH_2 , as-milled MgH_2 and

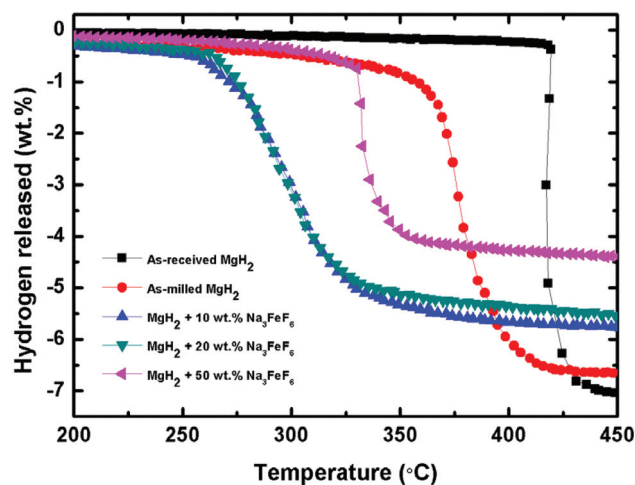


Fig. 1 TPD curves for the dehydrogenation of as-received MgH_2 , as-milled MgH_2 and the MgH_2 doped with 10 wt%, 20 wt% and 50 wt% Na_3FeF_6 under 1.0 atm vacuum with heating rate of 5 °C min^{-1} .

the MgH_2 with 10 wt%, 20 wt%, and 50 wt% Na_3FeF_6 added. From the results obtained, it was clearly shown that the TPD performance of MgH_2 was significantly improved by adding the Na_3FeF_6 nanopowder, resulting from the decrease of the onset dehydrogenation temperature of the doped sample as compared to the as-received and as-milled MgH_2 . The as-received MgH_2 started to release hydrogen at about 417 °C with a total dehydrogenation capacity of 7.1 wt% hydrogen after being heated to 450 °C (theoretically released at 7.6 wt% hydrogen). On the other hand, the onset desorption temperature of MgH_2 after milling was reduced to about 355 °C, which was 62 °C lower than the as-received MgH_2 with 6.7 wt% hydrogen. This result indicates that the onset desorption temperature of MgH_2 was also influenced by the milling process.^{20,43} This is supported by a study of the milled and un-milled MgH_2 within the scope of structural difference by Huot *et al.*¹⁶ They reported that the milled MgH_2 had faster hydrogen desorption kinetics and decreased activation energy compared to the un-milled MgH_2 . The graph also shows that the hydrogen desorption capacity of the MgH_2 after being milled was lower than of the as-received MgH_2 . This might occurred because of MgH_2 that released hydrogen during the milling process.

The addition of Na_3FeF_6 as a catalyst to the MgH_2 showed a decrease in the initial dehydrogenation temperature. After adding MgH_2 with 10 wt% Na_3FeF_6 , the sample started to release hydrogen at about 255 °C. For the MgH_2 doped with 20 wt% Na_3FeF_6 , the initial dehydrogenation temperature decreased to about 260 °C. From the results obtained, the onset desorption temperature of the doped MgH_2 with 10 wt% and 20 wt% Na_3FeF_6 samples were greatly enhanced by the reduction of about 100 and 95 °C, respectively compared with the as-milled MgH_2 , with the amount of hydrogen released reduced to about 5.7 and 5.5 wt% respectively. To further support the results obtained about the decrease of the onset desorption temperature of the doped sample, 50 wt% Na_3FeF_6 was added to the sample of MgH_2 . As expected, increasing the amount of dopant to 50 wt% Na_3FeF_6 improved the onset desorption temperature as compared with the as-milled MgH_2 by decreasing the temperature to about 330 °C with a total dehydrogenation capacity of only 4.4 wt%. This phenomenon is similar to a study reported by Wan *et al.* on NiFe_2O_4 doped MgH_2 .⁴⁴ They revealed that the reduction of hydrogen released in the $\text{MgH}_2 + 9 \text{ mol}\% \text{ NiFe}_2\text{O}_4$ as compared with the $\text{MgH}_2 + 3 \text{ mol}\% \text{ NiFe}_2\text{O}_4$ and $\text{MgH}_2 + 5 \text{ mol}\% \text{ NiFe}_2\text{O}_4$ was due to the excessive catalytic effects of the addition of excess NiFe_2O_4 . Barkhordarian *et al.*⁴⁵ also claimed the same condition in their study. They found that only 0.5 mol% Nb_2O_5 was sufficient to provide the fastest kinetics with a total dehydrogenation capacity of 7.0 wt%. These results suggest that Na_3FeF_6 played an important role as a catalyst in reducing the initial dehydrogenation temperature of the MgH_2 . In addition to Na_3FeF_6 , our previous study on complex metal fluoride catalysts, K_2TiF_6 ⁴⁶ and K_2ZrF_6 ,²² also showed an improvement in the onset dehydrogenation temperature of the doped sample as compared to the as-received and as-milled MgH_2 . All the samples started releasing hydrogen below 260 °C.

To further study the reversibility of MgH_2 after doping with Na_3FeF_6 , the isothermal rehydrogenation kinetics of the MgH_2 samples with and without the addition of Na_3FeF_6 was investigated at 320 °C and under 33.0 atm of H_2 , as shown in Fig. 2. The doped samples were studied at different ratios of Na_3FeF_6 : 10 wt%, 20 wt% and 50 wt%. Among the ratios studied, $\text{MgH}_2 + 10 \text{ wt}\% \text{ Na}_3\text{FeF}_6$ showed the fastest kinetics rate. Moreover, the hydrogen absorption properties of the $\text{MgH}_2 + 10 \text{ wt}\% \text{ Na}_3\text{FeF}_6$ composite was better than the un-doped composite. As shown in Fig. 2, the doped composite of 10 wt% Na_3FeF_6 can absorb about 3.6 wt% of H_2 in 2 min, whereas the as-milled MgH_2 only absorbed 3.0 wt% of hydrogen and required about 20 min to achieve the same capacity as the composite doped with 10 wt% Na_3FeF_6 . In addition, hydrogen absorbed was about 1.6 wt% and 1.2 wt% within 2 min after adding 20 wt% and 50 wt% Na_3FeF_6 , respectively. From the results, it can be seen that the hydrogen absorption behavior can be affected by the amount of the catalyst. This correlates with a study by Oelerich *et al.*³² who presented that the fastest sorption kinetics was obtained by using only 0.2 mol% of the catalyst. Ranjbar *et al.*⁴⁷ also reported that the reduction of the grain size of MgH_2 will enhance the kinetics results, but excess catalyst added to the sample would obstruct the hydrogen diffusion by blocking the diffusion paths. Taken together, Na_3FeF_6 can also be suggested as a good catalyst for the enhancement of rehydrogenation kinetics.

Fig. 3 presents the isothermal dehydrogenation kinetics of the as-milled MgH_2 and MgH_2 doped with 10 wt%, 20 wt% and 50 wt% Na_3FeF_6 , measured at 320 °C and under 1.0 atm of H_2 . As clearly shown in the graph, the sample with the Na_3FeF_6 catalyst showed a remarkable improvement compared to the un-doped sample. The 10 wt% Na_3FeF_6 -doped MgH_2 sample released about 3.8 wt% hydrogen in 10 min after 1 h of dehydrogenation. In comparison with our previous study,^{22,46} Na_3FeF_6 demonstrated better enhancement of desorption kine-

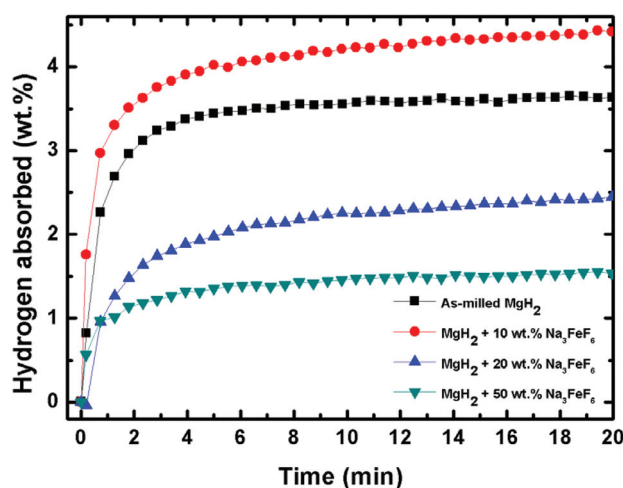


Fig. 2 Isothermal rehydrogenation kinetics of the dehydried samples of the as-milled MgH_2 and MgH_2 doped with 10 wt%, 20 wt% and 50 wt% Na_3FeF_6 at 320 °C and under 33.0 atm.

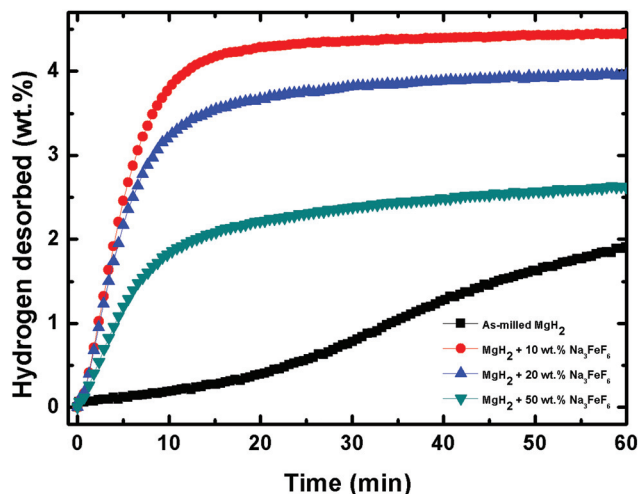


Fig. 3 Isothermal dehydrogenation kinetics of the rehydrated samples of the as-milled MgH_2 and the MgH_2 doped with 10 wt%, 20 wt% and 50 wt% Na_3FeF_6 at 320 °C and under 1.0 atm.

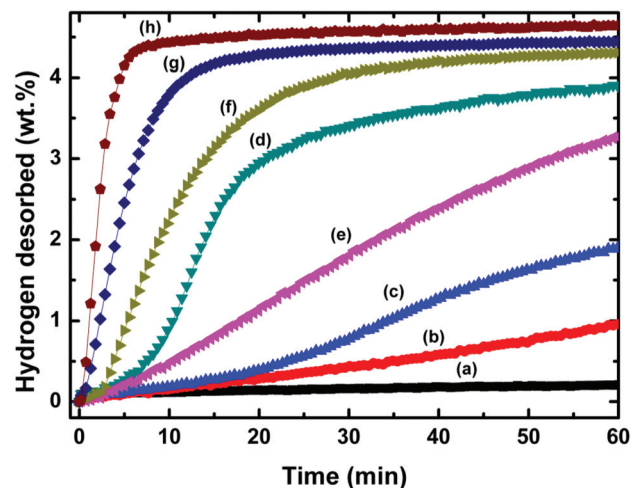


Fig. 4 Isothermal dehydrogenation curves of as-milled MgH_2 and MgH_2 doped with 10 wt% Na_3FeF_6 at 280 °C (a, e), 300 °C (b, f), 320 °C (c, g) and 340 °C (d, h).

tics than other complex metal fluoride catalysts (K_2TiF_6 and K_2ZrF_6). In 30 min, the $\text{MgH}_2 + 10 \text{ wt}\% \text{ Na}_3\text{FeF}_6$ sample released about 4.0 wt% hydrogen at 300 °C, whereas $\text{MgH}_2 + 10 \text{ wt}\% \text{ K}_2\text{TiF}_6$ and $\text{MgH}_2 + 10 \text{ wt}\% \text{ K}_2\text{ZrF}_6$ samples desorbed hydrogen at about 3.4 wt% and 3.0 wt%, respectively. MgH_2 doped with 20 wt% and 50 wt% Na_3FeF_6 released about 3.2 wt% and 1.8 wt% hydrogen in 10 min, respectively. In contrast, the as-milled MgH_2 sample desorbed only 0.2 wt% hydrogen in the same period of time. These results indicate that the Na_3FeF_6 catalyst also enhanced the dehydrogenation kinetics of MgH_2 .

From the results of the initial decomposition temperature and sorption kinetics, it was shown that the 10 wt% Na_3FeF_6 -doped MgH_2 sample was the best composite for the enhancement of the hydrogen storage properties of MgH_2 . Thus, the $\text{MgH}_2 + 10 \text{ wt}\% \text{ Na}_3\text{FeF}_6$ sample was chosen to investigate the mechanism and the catalytic effect on MgH_2 .

Fig. 4 compares the isothermal dehydrogenation kinetics of the un-doped MgH_2 and the $\text{MgH}_2 + 10 \text{ wt}\% \text{ Na}_3\text{FeF}_6$ sample at 280 °C, 300 °C, 320 °C and 340 °C. These dehydrogenation measurements were conducted at different temperatures under 1.0 atm pressure to further study the dehydrogenation kinetics of the as-milled MgH_2 and MgH_2 doped with 10 wt% Na_3FeF_6 . As displayed in the graph, MgH_2 doped with 10 wt% Na_3FeF_6 revealed a remarkable enhancement and better desorption kinetics compared to the un-doped MgH_2 . The $\text{MgH}_2 + 10 \text{ wt}\% \text{ Na}_3\text{FeF}_6$ sample released about 3.3 wt% hydrogen as shown in Fig. 4(e) in 60 min of dehydrogenation at 280 °C. There was a slight difference for the as-milled MgH_2 as the sample released only about 0.2 wt% hydrogen under the same conditions. Further heating the Na_3FeF_6 -doped MgH_2 sample at a higher temperature, as shown in Fig. 4(f)–(h), showed faster isothermal dehydrogenation kinetics than the un-doped sample. Under the same period, Na_3FeF_6 -doped MgH_2 released hydrogen to about 4.3 wt%, 4.5 wt% and 4.7 wt% at 300 °C, 320 °C and 340 °C, respectively. On the other hand, the

as-milled MgH_2 released about 1.0 wt%, 1.9 wt% and 3.9 wt% under the same conditions (Fig. 4(b)–(d)). These results show that the improvement of the desorption kinetics of MgH_2 can be achieved by doping with Na_3FeF_6 . This kinetic enhancement was related to the energy barrier of the H_2 release from MgH_2 .

In the present study, adding Na_3FeF_6 to the MgH_2 reduced the activation energy for the decomposition of MgH_2 . The Arrhenius equation shown below was used to calculate the apparent activation energy, E_A of the as-milled MgH_2 and $\text{MgH}_2 + 10 \text{ wt}\% \text{ Na}_3\text{FeF}_6$.

$$k = k_0 \exp(-E_A/RT) \quad (1)$$

where k is the rate of dehydrogenation, k_0 is a temperature independent coefficient, E_A is the apparent activation energy for hydride decomposition, R is the gas constant, and T is the absolute temperature. As shown in Fig. 5, by plotting $\ln(k)$ vs. $1/T$, the apparent activation energies, E_A , for hydrogen to be released from the un-doped MgH_2 and $\text{MgH}_2 + 10 \text{ wt}\% \text{ Na}_3\text{FeF}_6$ were identified. From the calculations, the activation energy, E_A , for the decomposition of $\text{MgH}_2 + 10 \text{ wt}\% \text{ Na}_3\text{FeF}_6$ sample was about $75.0 \pm 0.4 \text{ kJ mol}^{-1}$, which was about 92.0 kJ mol^{-1} lower than for the as-milled MgH_2 ($167.0 \pm 1.4 \text{ kJ mol}^{-1}$). In our previous studies,^{22,46} it was shown that the activation energy for the hydrogen desorption of MgH_2 doped with 10 wt% K_2ZrF_6 was 80 kJ mol^{-1} and 132 kJ mol^{-1} for the $\text{MgH}_2 + 10 \text{ wt}\% \text{ K}_2\text{TiF}_6$ sample. Therefore, this study has shown that doping MgH_2 with Na_3FeF_6 has even lower desorption activation energy, demonstrating the superiority of Na_3FeF_6 in enhancing the dehydrogenation properties of magnesium hydride, as compared with other complex metal fluoride catalysts such as K_2TiF_6 and K_2ZrF_6 . These results were supported by a study which claimed that the reduction of the activation energy was due to the use of various catalysts, especially any transition metal additive that leads to the provision of a site for the hydrogen dissociation and recombina-

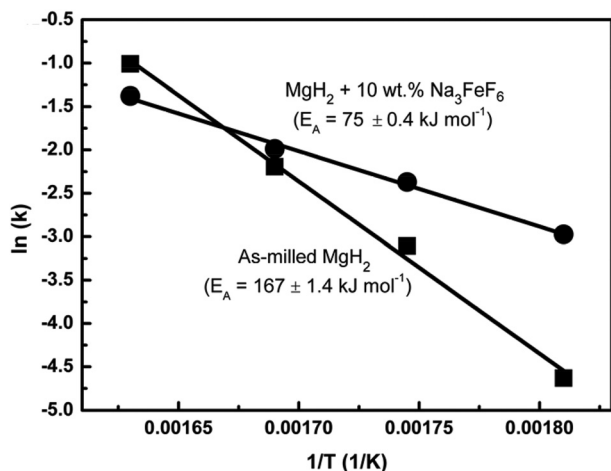


Fig. 5 Arrhenius plots of $\ln(k)$ vs. $1/T$ for as-milled MgH_2 and MgH_2 doped with 10 wt% Na_3FeF_6 .

tion during the absorption and desorption processes. Ball milling is also one of the best ways to lower the activation energy because of the fresh un-oxidized surfaces that result from the breaking up of the Mg or MgH_2 powder particles;⁴⁸ thus, the decrease of the activation energy enhances the sorption properties of MgH_2 .

The thermal properties of the as-milled MgH_2 and $\text{MgH}_2 + 10$ wt% Na_3FeF_6 samples were further investigated by DSC, with the results shown in Fig. 6. Clearly, the curve for the as-milled MgH_2 shows only one strong endothermic process, namely, a peak at 440.30 °C that corresponds to the decomposition of the MgH_2 . In addition, the DSC curves for the $\text{MgH}_2 + 10$ wt% Na_3FeF_6 sample are similar to those of the as-milled MgH_2 sample, displaying only one endothermic peak at 342.76, which corresponds to the decomposition of MgH_2 but with the peaks having moved to lower temperatures. Further-

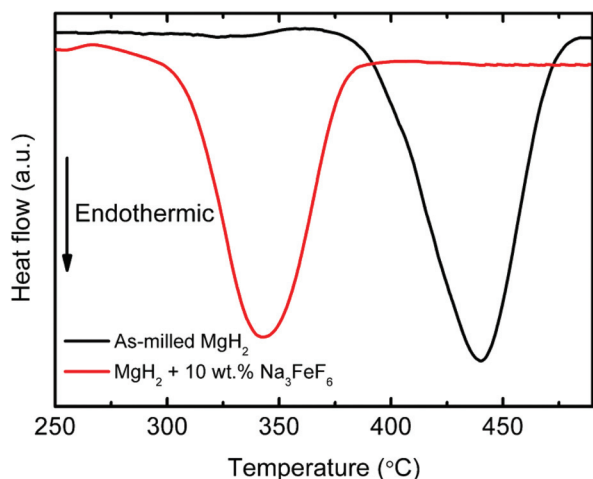


Fig. 6 DSC traces of the as-milled MgH_2 and $\text{MgH}_2 + 10$ wt% Na_3FeF_6 (heating rate: 20 °C min^{-1} ; argon flow: 30 mL min^{-1}).

more, it can be seen that the onset decomposition temperatures of the samples in DSC were slightly higher than in the TPD (Fig. 1). These differences may result from the fact that dehydrogenation was conducted under different heating rates and atmospheres in two types of measurements. The DSC measurement was run under 1.0 atm argon flow with a heating rate of 20 °C min^{-1} , while the TPD measurement was conducted under the condition of 1.0 atm vacuum with 5 °C min^{-1} heating rate, resulting in different driving forces during the desorption process. A similar phenomenon has also been reported in our previous studies.^{49,50}

In order to determine the hydrogen desorption enthalpy (ΔH_{dec}) of MgH_2 decomposition, the DSC curves were analyzed by the STARE software and the hydrogen desorption enthalpy was obtained from the integrated peak areas. The hydrogen desorption enthalpy for as-milled MgH_2 was calculated as 75.2 kJ mol^{-1} H_2 , which is almost the same as the theoretical value (76 kJ mol^{-1} H_2). After the addition of Na_3FeF_6 , the enthalpy of hydrogen desorption of MgH_2 was similar to that of un-doped MgH_2 . These results indicate that the additive investigated in this study acted as a catalyst and did not change the thermodynamics of the system (destabilization effect). This phenomenon is similar to previous reports on metal halide doped MgH_2 .^{51,52} However, other studies have reported that both the thermodynamic and kinetic properties of MgH_2 could be adjusted at the same time with the addition of a catalyst.^{44,53}

Fig. 7 displays the SEM images of the as-received MgH_2 , as-received Na_3FeF_6 , as-milled MgH_2 and 10 wt% Na_3FeF_6 -doped MgH_2 . From the SEM images, the un-milled MgH_2 sample had the largest particle size compared to the milled sample. As shown in Fig. 7(a), the as-received MgH_2 sample had an angular shape with a particle size that was larger than 100 μm . Fig. 7(b) shows the Na_3FeF_6 sample with particle size smaller than 5 μm . After undergoing the ball milling process for 1 h, the particle size of the MgH_2 sample, as shown in Fig. 7(c), became inhomogeneous. The average size of the MgH_2 particles also caused a drastic decrease with some agglomeration. On the other hand, it is clearly shown in Fig. 7(d) that the particle size of the MgH_2 doped with 10 wt% Na_3FeF_6 as a catalyst had the smallest size compared with the as-received and as-milled MgH_2 . This might be due to the hardness of the Na_3FeF_6 , which helped MgH_2 to break into a smaller size. This phenomenon is similar to that in our previous report on complex metal fluoride catalysts, K_2TiF_6 and K_2ZrF_6 doped MgH_2 ,^{22,46} in which the hardness of the additive helped to break the MgH_2 particles into smaller sizes. The small size of the particles leads to the enhancement of hydrogen absorption/desorption. The minimum initial dehydrogenation temperature is also improved with the rise of the specific surface area and decrease of the diffusion length of hydrogen.⁵⁴

XRD was used to analyze the phase structure of the MgH_2 doped with 10 wt% Na_3FeF_6 after 1 h of ball milling after dehydrogenation at 450 °C and after rehydrogenation at 320 °C under 33.0 atm hydrogen pressure, as shown in Fig. 8. After 1 h of ball milling, only MgH_2 peaks were observed; no peaks

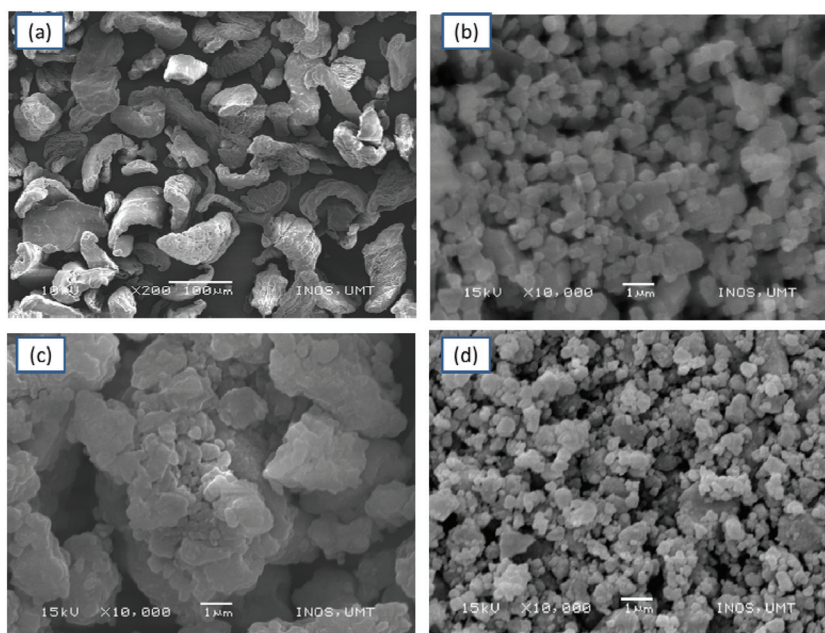


Fig. 7 The SEM images of the (a) as-received MgH_2 , (b) as-received Na_3FeF_6 , (c) as-milled MgH_2 and (d) $\text{MgH}_2 + 10 \text{ wt}\% \text{ Na}_3\text{FeF}_6$.

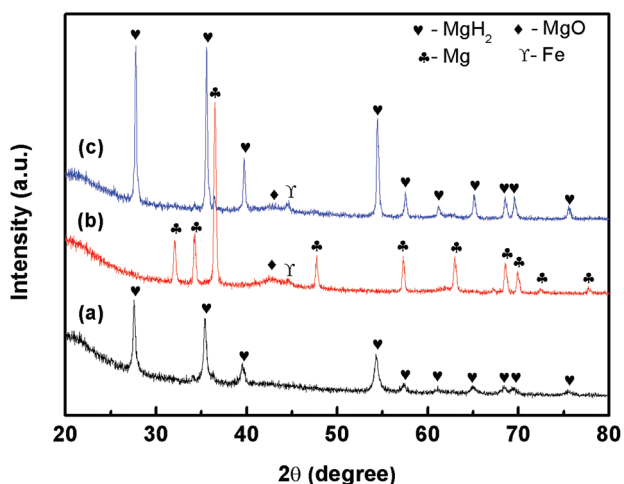


Fig. 8 XRD patterns of MgH_2 doped with 10 wt% Na_3FeF_6 (a) after ball milling for 1 h, (b) after dehydrogenation at 450 °C and (c) after rehydrogenation at 320 °C.

of Na_3FeF_6 were found as clearly shown in Fig. 8(a). The reason the parent material of Na_3FeF_6 -containing phases was not detected could be because of its transformation into an amorphous state after undergoing the milling process or possibly due to the fact that the amount of Na_3FeF_6 was too small to be detected by the XRD machine. After dehydrogenation at 450 °C, as shown in Fig. 8(b), there were distinct peaks of Mg, which revealed that MgH_2 was fully transformed to Mg, thus indicating the completion of the dehydrogenation of MgH_2 , as shown in the equation below:



Moreover, a peak of Fe could be seen after the dehydrogenation. In addition, the MgO phase was also detected in the dehydrogenation, due to contamination with a little oxygen, which occurred during the sample preparation because of the reaction between Mg and oxygen. Fig. 8(c) displays the results for the rehydrogenated sample. Major peaks of Mg were detected, showing that the Mg phase was largely transformed into MgH_2 ; the peaks of Fe and MgO were still present. The reaction that occurred between MgH_2 and Na_3FeF_6 during the ball milling or heating process may have been caused by the appearance of the active species of Fe after the de/rehydrogenation processes.

To further explore the Na_3FeF_6 -containing phase after dehydrogenation and after rehydrogenation, a sample of MgH_2 with 20 wt% Na_3FeF_6 was prepared. Fig. 9 presents the XRD patterns of the MgH_2 doped with 20 wt% Na_3FeF_6 after 1 h of milling, after dehydrogenation at 450 °C and after rehydrogenation at 320 °C under the hydrogen pressure of 33.0 atm. After undergoing the 1 h ball milling process, as shown in Fig. 9(a), it can be seen that only the parent materials, MgH_2 and Na_3FeF_6 , were detected in the XRD pattern. No new compounds were formed at this stage. As can be clearly seen in the graph, the peaks of the catalyst can be detected in the milled reactant of MgH_2 doped with 20 wt% Na_3FeF_6 compared to the MgH_2 doped with 10 wt% Na_3FeF_6 . The results indicate that the amount of 20 wt% Na_3FeF_6 was large enough to be deemed as detectable by the XRD machine. After heating to 450 °C, the peaks of MgH_2 and Na_3FeF_6 disappeared, as can be seen in Fig. 9(b). The results show that MgH_2 was fully transformed into Mg. In addition, the phase structures of Fe and MgO were still present, together with some new peaks of NaMgF_3 and NaF observed after the dehydrogenation process,

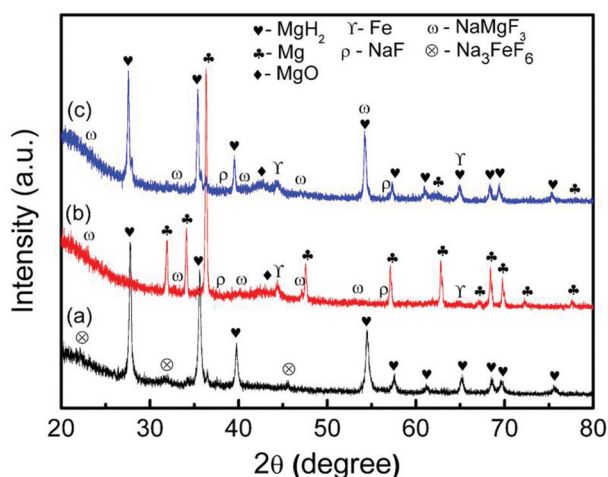


Fig. 9 XRD patterns of MgH_2 doped with 20 wt% Na_3FeF_6 (a) after ball milling for 1 h, (b) after dehydrogenation at 450 °C and (c) after rehydrogenation at 320 °C.

proposing that a reaction might partially take place during the heating process between MgH_2 and Na_3FeF_6 as stated below:



The values of the standard Gibbs free energy, ΔG_f° , of MgH_2 , Na_3FeF_6 , NaMgF_3 and NaF are -35.98 , -2606.23 , -1616.28 , and $-545.18 \text{ kJ mol}^{-1}$,⁵⁵ respectively. Thus, $-1163.98 \text{ kJ mol}^{-1}$ would be the total change in ΔG° for MgH_2 . The standard-state free energy of the reaction, ΔG° , was calculated using the equation stated below:

$$\Delta G^\circ = \sum \Delta G_{f,\text{products}}^\circ - \Delta G_{f,\text{reactions}}^\circ \quad (4)$$

The possibility of the reaction as stated in eqn (3) was proven by the results obtained from the thermodynamic potentials. Moreover, Fig. 9(c) shows the XRD pattern of the rehydrogenated sample. From these results, it can be seen that the Mg phase was largely transformed into MgH_2 , but minor peaks of Mg were still present, indicating that MgH_2 formation was not fully reversible in the rehydrogenation phase. The peaks of NaMgF_3 , NaF , Fe , and MgO still existed. The appearance of the F-containing catalytic species, NaMgF_3 and NaF in the XRD spectra for the dehydrogenated and rehydrogenated samples might be detected due to higher concentrations after the amount of catalyst added was increased to 20 wt%, as compared to the sample of $\text{MgH}_2 + 10 \text{ wt% Na}_3\text{FeF}_6$ with no detection of F species observed, shown in Fig. 8.

Following the first complete cycle (de/rehydrogenation), the samples were subjected to a second dehydrogenation under 1.0 atm hydrogen pressure at 320 °C. Fig. 10 shows the XRD patterns of the MgH_2 doped with 20 wt% Na_3FeF_6 after the second dehydrogenation. Compared with the mixed sample after the first dehydrogenation, NaMgF_3 , NaF and Fe phases did not change, indicating that the ternary combination (NaMgF_3 , NaF and Fe) is very stable. Therefore, Na_3FeF_6 plays a role in just the first MgH_2 dehydrogenation. In the next hydrid-

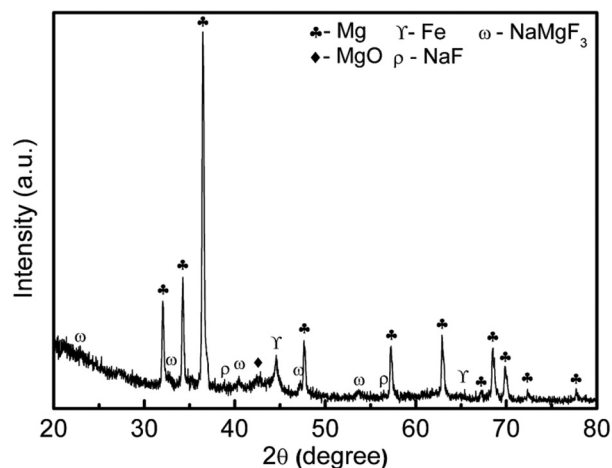


Fig. 10 XRD patterns of MgH_2 doped with 20 wt% Na_3FeF_6 after second dehydrogenation kinetics at 320 °C and under 1.0 atm.

ing-dehydriding cycles, NaMgF_3 , NaF and Fe are the main phases that affect the hydrogen storage properties of MgH_2 , and the second dehydrogenation can be expected to be similar to reaction (2).

The results obtained show that the formation of the *in situ* active species of NaMgF_3 , NaF and Fe , which resulted from the reaction of MgH_2 and Na_3FeF_6 during the dehydrogenation process, could play an important role in improving the hydrogen sorption of MgH_2 . The formation of the active species of NaMgF_3 and NaF indicated that the Na_3FeF_6 component in the MgH_2 - Na_3FeF_6 sample played a catalytic role through the formation of F-containing catalytic species. This finding is correlated with the previous work that studied the effects of transition metal fluorides on the hydrogen storage properties of MgH_2 , as reported by Jin *et al.*⁵⁶ They revealed that the reaction between MgH_2 and transition metal fluorides during milling and hydrogenation had formed the hydride phases that could play a real role in enhancing the hydrogenation kinetics of MgH_2 . From the study, many of the fluorides displayed significant catalytic effects in terms of onset desorption temperature and de/rehydrogenation kinetics of MgH_2 . In addition, the improvement of the dehydrogenation properties of alanate was also proven and it was influenced by the F-containing catalytic species.³⁷ Moreover, NaF was one of the active species that helped in the enhancement of the hydrogen storage in NaAlH_4 with synergetic catalysis.⁴⁰ NaF particles were also reported to work as a nucleation centre, which promoted the nucleation and growth of NaH in the dehydrogenation process, resulting from the identical crystallographic structure and comparable lattice parameters.⁴²

The formation of the *in situ* Fe particles resulting from the reaction of MgH_2 and Na_3FeF_6 during the dehydrogenation process may play an important role in the enhancement of MgH_2 storage properties, because it is well-known that Fe is a good catalyst for MgH_2 .^{35,57} Fe may interact with hydrogen molecules, which may lead to the dissociation of the hydrogen

molecules and the enhancement of the sorption kinetics. On the other hand, it has been reported that the formation/decomposition of MgH_2 on the dissociation/recombination of the hydrogen molecule was caused by the catalytic effects of Fe.^{58–60} From the previous studies, it was clearly shown that the F-containing catalytic species and Fe-species can act as a great catalyst for MgH_2 . Therefore, based on the results obtained, the excellent dehydrogenation properties of MgH_2 were achieved because of the newly developed ternary combination of NaMgF_3 , NaF and Fe , which acted as a real catalyst in the reaction during the dehydrogenation process. The *in situ* ternary combination (NaMgF_3 , NaF and Fe) served as an active species and played a synergistic role, which improved the hydrogen storage properties of the Na_3FeF_6 -doped MgH_2 sample.

4. Conclusion

In conclusion, by doping with Na_3FeF_6 , the hydrogen storage performance of MgH_2 has been significantly improved. MgH_2 doped with 10 wt% Na_3FeF_6 achieved optimal sorption performance, including the initial dehydrogenation temperature and the isothermal de/rehydrogenation kinetics. An onset dehydrogenation temperature of 255 °C was observed for the 10 wt% Na_3FeF_6 doped MgH_2 , decreasing the desorption temperature by about 100 °C compared to the un-doped MgH_2 sample. In terms of the isothermal rehydrogenation kinetics, the MgH_2 sample doped with 10 wt% Na_3FeF_6 absorbed about 3.6 wt% of hydrogen at 320 °C in 2 min of rehydrogenation, whereas the as-milled MgH_2 only absorbed 3.0 wt% of hydrogen and required about 20 min to achieve the same capacity as the doped sample. On the other hand, for the isothermal dehydrogenation kinetics, the MgH_2 sample doped with 10 wt% Na_3FeF_6 released about 3.8 wt% hydrogen in 10 min, whereas the as-milled MgH_2 sample desorbed only 0.2 wt% of hydrogen in the same period of time. Moreover, the apparent activation energy, E_A , for the decomposition of $\text{MgH}_2 + 10$ wt% Na_3FeF_6 was decreased from 167.0 kJ mol^{-1} for the as-milled MgH_2 to 75.0 kJ mol^{-1} . From this study, it is reasonable to conclude that the *in situ* active species of NaMgF_3 , NaF and Fe that were formed by the doping of MgH_2 with Na_3FeF_6 during the heating process acted as a real catalyst in enhancing the hydrogen storage properties of MgH_2 .

Acknowledgements

The authors would like to express gratitude to the Universiti Malaysia Terengganu for providing the facilities to carry out this project. The authors also acknowledge the Ministry of Higher Education Malaysia for financial support through the Fundamental Research Grant Scheme (FRGS 59362). N. N. Sulaiman and N.S. Mustafa are thankful to the Ministry of Education Malaysia for the 'My Brain15' scholarship.

References

- 1 B. Sakintuna, F. Lamari-Darkrim and M. Hirscher, *Int. J. Hydrogen Energy*, 2007, **32**, 1121–1140.
- 2 S. Srinivasa Murthy and E. Anil Kumar, *Appl. Therm. Eng.*, 2014, **72**, 176–189.
- 3 F. Cuevas, D. Korablov and M. Latroche, *Phys. Chem. Chem. Phys.*, 2012, **14**, 1200–1211.
- 4 L. Mooij and B. Dam, *Phys. Chem. Chem. Phys.*, 2013, **15**, 11501–11510.
- 5 P. Dantzer, *Mater. Sci. Eng. A*, 2002, **329–331**, 313–320.
- 6 J. Huang, Y. Yan, A. Remhof, Y. Zhang, D. Rentsch, Y. S. Au, P. E. de Jongh, F. Cuevas, L. Ouyang, M. Zhu and A. Zuttel, *Dalton Trans.*, 2016, **45**, 3687–3690.
- 7 L. Li, Y. Xu, Y. Wang, Y. Wang, F. Qiu, C. An, L.-F. Jiao and H. Yuan, *Dalton Trans.*, 2013, **43**, 1806–1813.
- 8 M. Ismail, Y. Zhao, X. B. Yu and S. X. Dou, *Int. J. Hydrogen Energy*, 2010, **35**, 2361–2367.
- 9 Y. Zhang, Q. Tian, J. Zhang, S.-S. Liu and L.-X. Sun, *J. Phys. Chem. C*, 2009, **113**, 18424–18430.
- 10 X. B. Yu, Y. H. Guo, D. L. Sun, Z. X. Yang, A. Ranjbar, Z. P. Guo, H. K. Liu and S. X. Dou, *J. Phys. Chem. C*, 2010, **114**, 4733–4737.
- 11 M. Ismail, Y. Zhao, X. B. Yu, I. P. Nevirkovets and S. X. Dou, *Int. J. Hydrogen Energy*, 2011, **36**, 8327–8334.
- 12 Y. Zhang, W.-S. Zhang, A.-Q. Wang, S. Li-Xian, M.-Q. Fan, H.-L. Chu, J.-C. Sun and T. Zhang, *Int. J. Hydrogen Energy*, 2007, **32**, 3976–3980.
- 13 C.-Y. Wang, C.-S. Tsao, M.-S. Yu, P.-Y. Liao, T.-Y. Chung, H.-C. Wu, M. A. Miller and Y.-R. Tzeng, *J. Alloys Compd.*, 2010, **492**, 88–94.
- 14 H. Imamura, K. Yoshihara, M. Yoo, I. Kitazawa, Y. Sakata and S. Ooshima, *Int. J. Hydrogen Energy*, 2007, **32**, 4191–4194.
- 15 J. Mao, Z. Guo, X. Yu, H. Liu, Z. Wu and J. Ni, *Int. J. Hydrogen Energy*, 2010, **35**, 4569–4575.
- 16 J. Huot, G. Liang, S. Boily, A. Van Neste and R. Schulz, *J. Alloys Compd.*, 1999, **293–295**, 495–500.
- 17 H. Chu, S. Qiu, L. Sun and J. Huot, *Dalton Trans.*, 2015, **44**, 16694–16697.
- 18 M. Ismail, *Energy*, 2015, **79**, 177–182.
- 19 A. Ranjbar, M. Ismail, Z. P. Guo, X. B. Yu and H. K. Liu, *Int. J. Hydrogen Energy*, 2010, **35**, 7821–7826.
- 20 H. Gasan, O. N. Celik, N. Aydinbeyli and Y. M. Yaman, *Int. J. Hydrogen Energy*, 2012, **37**, 1912–1918.
- 21 N. Juahir, N. S. Mustafa, A. Sinin and M. Ismail, *RSC Adv.*, 2015, **5**, 60983–60989.
- 22 F. A. Halim Yap, N. S. Mustafa and M. Ismail, *RSC Adv.*, 2015, **5**, 9255–9260.
- 23 L. Z. Ouyang, X. S. Yang, M. Zhu, J. W. Liu, H. W. Dong, D. L. Sun, J. Zou and X. D. Yao, *J. Phys. Chem. C*, 2014, **118**, 7808–7820.
- 24 L. Z. Ouyang, Z. J. Cao, H. Wang, J. W. Liu, D. L. Sun, Q. A. Zhang and M. Zhu, *Int. J. Hydrogen Energy*, 2013, **38**, 8881–8887.
- 25 L. Z. Ouyang, F. X. Qin and M. Zhu, *Scr. Mater.*, 2006, **55**, 1075–1078.

- 26 H. Liu, C. Wu, H. Zhou, T. Chen, Y. Liu, X. Wang, Z. Dong, H. Ge, S. Li and M. Yan, *RSC Adv.*, 2015, **5**, 22091–22096.
- 27 S. Kurko, A. Aurora, D. M. Gattia, V. Contini, A. Montone, Ž. Rašković-Lovre and J. G. Novaković, *Int. J. Hydrogen Energy*, 2013, **38**, 12140–12145.
- 28 M. Ismail, Y. Zhao and S. X. Dou, *Int. J. Hydrogen Energy*, 2013, **38**, 1478–1483.
- 29 L. Zaluski, A. Zaluska and J. O. Ström-Olsen, *J. Alloys Compd.*, 1997, **253–254**, 70–79.
- 30 B. Bogdanović and M. Schwickardi, *J. Alloys Compd.*, 1997, **253–254**, 1–9.
- 31 M. Ismail, Y. Zhao, X. B. Yu, J. F. Mao and S. X. Dou, *Int. J. Hydrogen Energy*, 2011, **36**, 9045–9050.
- 32 W. Oelerich, T. Klassen and R. Bormann, *J. Alloys Compd.*, 2001, **315**, 237–242.
- 33 C. X. Shang, M. Bououdina, Y. Song and Z. X. Guo, *Int. J. Hydrogen Energy*, 2004, **29**, 73–80.
- 34 J. L. Bobet, E. Akiba, Y. Nakamura and B. Darriet, *Int. J. Hydrogen Energy*, 2000, **25**, 987–996.
- 35 G. Liang, J. Huot, S. Boily, A. Van Neste and R. Schulz, *J. Alloys Compd.*, 1999, **292**, 247–252.
- 36 L.-P. Ma, P. Wang and H.-M. Cheng, *Int. J. Hydrogen Energy*, 2010, **35**, 3046–3050.
- 37 L.-C. Yin, P. Wang, X.-D. Kang, C.-H. Sun and H.-M. Cheng, *Phys. Chem. Chem. Phys.*, 2007, **9**, 1499–1502.
- 38 H. W. Brinks, A. Fossdal and B. C. Hauback, *J. Phys. Chem. C*, 2008, **112**, 5658–5661.
- 39 Y. Liu, F. Wang, Y. Cao, M. Gao, H. Pan and Q. Wang, *Energy Environ. Sci.*, 2010, **3**, 645–653.
- 40 Y. Liu, C. Liang, H. Zhou, M. Gao, H. Pan and Q. Wang, *Chem. Commun.*, 2011, **47**, 1740–1742.
- 41 N. Juahir, N. S. Mustafa, F. A. Halim Yap and M. Ismail, *Int. J. Hydrogen Energy*, 2015, **40**, 7628–7635.
- 42 S. Singh and S. W. H. Eijt, *Phys. Rev. B: Condens. Matter*, 2008, **78**, 224110.
- 43 R. A. Varin, M. Jang, T. Czujko and Z. S. Wronski, *J. Alloys Compd.*, 2010, **493**, L29–L32.
- 44 Q. Wan, P. Li, J. Shan, F. Zhai, Z. Li and X. Qu, *J. Phys. Chem. C*, 2015, **119**, 2925–2934.
- 45 G. Barkhordarian, T. Klassen and R. Bormann, *J. Alloys Compd.*, 2004, **364**, 242–246.
- 46 N. S. Mustafa and M. Ismail, *Int. J. Hydrogen Energy*, 2014, **39**, 15563–15569.
- 47 A. Ranjbar, Z. Guo, X. Yu, D. Wexler, A. Calka, C. Kim and H. Liu, *Mater. Chem. Phys.*, 2009, **114**, 168–172.
- 48 C. J. Webb, *J. Phys. Chem. Solids*, 2015, **84**, 96–106.
- 49 M. Ismail, N. Juahir and N. S. Mustafa, *J. Phys. Chem. C*, 2014, **118**, 18878–18883.
- 50 M. Ismail, N. S. Mustafa, N. Juahir and F. A. H. Yap, *Mater. Chem. Phys.*, 2016, **170**, 77–82.
- 51 S.-A. Jin, J.-H. Shim, J.-P. Ahn, Y. W. Cho and K.-W. Yi, *Acta Mater.*, 2007, **55**, 5073–5079.
- 52 I. E. Malka, M. Pisarek, T. Czujko and J. Bystrzycki, *Int. J. Hydrogen Energy*, 2011, **36**, 12909–12917.
- 53 L. Z. Ouyang, Z. J. Cao, H. Wang, J. W. Liu, D. L. Sun, Q. A. Zhang and M. Zhu, *J. Alloys Compd.*, 2014, **586**, 113–117.
- 54 H. Gasan, N. Aydinbeyli, O. N. Celik and Y. M. Yaman, *J. Alloys Compd.*, 2009, **487**, 724–729.
- 55 <http://www.drjez.com/uco/.../StandardThermodynamicValues>.
- 56 S.-A. Jin, J.-H. Shim, Y. W. Cho and K.-W. Yi, *J. Power Sources*, 2007, **172**, 859–862.
- 57 N. Hanada, T. Ichikawa and H. Fujii, *J. Phys. Chem. B*, 2005, **109**, 7188–7194.
- 58 A. Bläsius and U. Gonster, *Appl. Phys.*, 1980, **22**, 331–332.
- 59 J. M. Welter and P. S. Rudman, *Scr. Metall.*, 1982, **16**, 285–286.
- 60 M. Ismail, *Int. J. Hydrogen Energy*, 2014, **39**, 2567–2574.